Capturing the life history of the marine copepod *Calanus sinicus* into a generic bioenergetics framework*

Tjalling Jager[a,*], Iurgi Salaberria[b], Bjørn Henrik Hansen[b]

[a] *Dept. of Theoretical Biology, VU University Amsterdam, de Boelelaan 1085, NL-1081 HV, Amsterdam, the Netherlands*
[b] *SINTEF Materials and Chemistry, Marine Environmental Technology, N-7465 Trondheim, Norway*

Abstract

Quantitative knowledge about copepod life histories is of crucial importance to interpret and predict the impacts of natural and anthropogenic stressors in this taxonomic group. Dynamic Energy Budget (DEB) models are a useful tool in this context, as they quantitatively link the energy taken up by feeding to energy-demanding traits such as growth, development and reproduction. The copepod life cycle, however, has several features that require closer investigation. Firstly, they sport larval development through six naupliar stages (of which the initial stages do not feed), followed by six copepodite stages (which have a different shape from the nauplii). Furthermore, growth stops rather abruptly after the final moult to the adult stage, and many species build up a large lipid storage to survive, and initiate reproduction, in absence of food. After a few modifications, the simple and generic DEBkiss model could be calibrated for *Calanus sinicus* using data on body composition and size at age for different temperatures. Embryo and naupliar development were well explained by the model, after correcting for

*Tel.: +31 20 5987134; fax: +31 20 5987123
Email address: tjalling.jager@vu.nl (Tjalling Jager)
URL: http://www.debtox.info/ (Tjalling Jager)

their deviating shape from the copepodites. Ceasing of growth after the final moult was implemented as a size-dependent switch in allocation. With these assumptions, predictions could be made for the rates of ingestion, respiration and reproduction in adults. The predictions were consistent with observed rates, which indicates the realism of the model structure and its parameterisation. Several issues remain to be addressed, specifically, the dynamics of lipid storage and its use. However, the present study provides a starting point for applications of DEB theory to copepods.

Keywords: Dynamic Energy Budget, DEBkiss, *Calanus sinicus*, life-history traits, parameter estimation, copepods

---

1. Introduction

Copepods form a major part of the zooplankton, and thereby play a crucial role in marine food webs. To predict the population consequences of natural and anthropogenic stresses, quantitative knowledge about their life histories is essential. To structure our ideas about the quantitative aspects of life histories, the most useful starting point are the conservation laws for mass and energy. Individual traits like growth and reproduction, as well as the costs to maintain the body, are energy-demanding processes, which ultimately need to be fuelled from feeding. It is these allocation rules that shape the life history of the species from egg to death. The theory of Dynamic Energy Budgets (DEB) provides a general framework for metabolic organisation, and thereby specifies the rules for the acquisition and use of energy that individual organisms follow over their entire life cycle (Kooijman, 2001; Nisbet et al., 2000). This theory has been applied extensively to interpret and predict the effects of stressors such as toxicants (e.g., Jager et al., 2014a), and to predict life histories under different environmental scenarios (e.g., Saraiva et al., 2012). The fact that DEB is a generic theory is of great help in these applications, as we do not have to build a new model from scratch for each species.

The potential for application of DEB theory to marine copepods was already qualitatively discussed by Klok et al. (2012), with special reference to the consequences of oil pollution in the Arctic. Quantitative DEB analysis can, however, be challenging and generally requires a comprehensive data set on a species, although theoretical considerations can be used to fill data gaps (Lika et al., 2011). Recently, a simplified energy-budget framework

was presented under the name DEBkiss (Jager et al., 2013), which allows straightforward parameterisation on limited data sets, while adhering to a strict mass balance. This model has previously been used to interpret the effects of toxic stress for such different species as the pond snail *Lymnaea stagnalis* (Barsi et al., 2014), the nematode *Caenorhabditis elegans* (Jager et al., 2014b), the springtail *Folsomia candida* (Hamda, 2014), and Antarctic krill *Euphausia superba* (Jager and Ravagnan, Acc.).

The life history of copepods deviates on several points from the life cycle of the 'standard' animal in DEB models (Kooijman, 2001; Nisbet et al., 2000). All copepods go through a fixed number of moults, and growth ceases rather abruptly after the final moult; determinate growth, which is also observed in several other crustacean groups (see Hartnoll, 2001) and most insects. This contrasts the von Bertalanffy growth pattern that is seen in most animals (and which arises from standard DEB models), where growth smoothly slows down as the individual approaches an asymptotic maximum size (see e.g., Nisbet et al., 2000). After hatching, copepods go through six nauplius larval stages (NI-NVI), which have a different shape than the later six copepodite stages (CI-CVI), and the first few stages do not feed (generally, NI and NII). Many copepod species build up a large lipid storage, which can be used to sustain the animal under food limitation and diapause, and can also fuel gonad development and egg production (Lee et al., 2006). Clearly, these issues require modification of the basic DEBkiss model. DEB theory is a theory for all living organisms, and metabolic rules are shaped by evolution. This limits our freedom to modify the model; it is unlikely that copepods have a radically different metabolic organisation from the other animals to which they are related. Therefore, we need to depart from the standard DEB structure, and develop logical and plausible adaptations that might have evolved to yield the copepod life history.

Here, we modify, parameterise and test the DEBkiss model for the calanoid copepod *Calanus sinicus*, which occurs in shelf waters around China, Japan and Korea. For this species, a detailed data set is available on growth and development, under controlled laboratory conditions, at different temperatures (Uye, 1988). The objective of this study is, however, broader than this particular species: to adapt a generic energy-budget model to serve as a baseline model for calanoid copepods in general. In future research, this model can be used for interpreting and predicting the effects of stressors (such as toxicants and climate change) on the life cycle of marine copepods, and on their population dynamics.

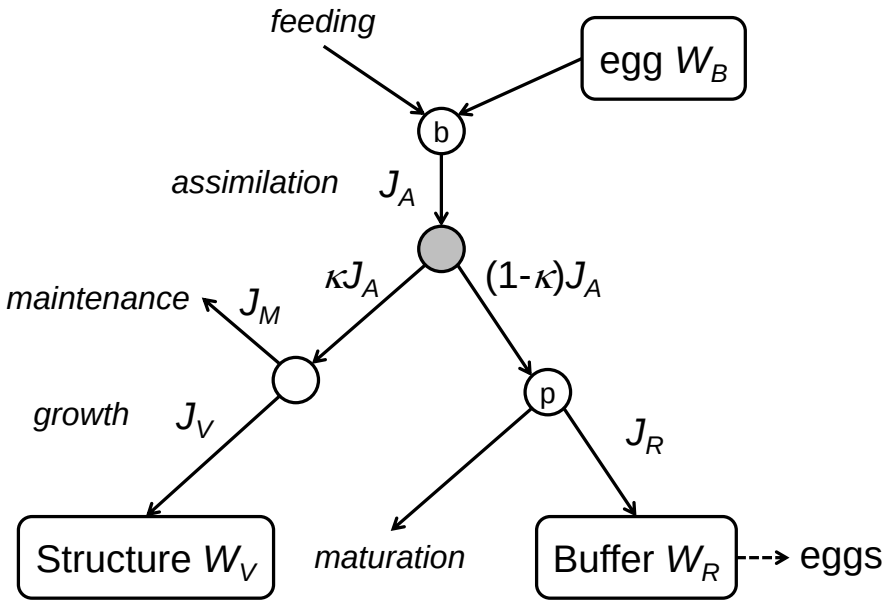

Figure 1: Schematic diagram of the energy flows in a standard DEBkiss animal. The nodes b and p denote switches at birth (start of feeding) and puberty (start of reproductive investment). The mobilisation flux is split according to a constant fraction κ.

2. Methods

2.1. Basic DEBkiss model

The DEBkiss model, including the underlying assumptions, is discussed in detail in Jager et al. (2013). The mass flows in the basic model are schematically drawn in Figure 1, and the model equations and conversions are provided in Table 1. Model parameters are explained in Table 2.

Briefly, assimilates are obtained from feeding or from the egg buffer (in embryo and non-feeding larval stages) provided by the mother. The link between food availability and feeding rates is condensed into a scaled functional response, f, such that $f = 0$ represent complete starvation and $f = 1$ *ad libitum* feeding conditions. A constant fraction κ of the assimilation flux is used for the soma (structural growth and maintenance). Maintenance costs are paid first, and the remaining flux can be used for growth. The other fraction of assimilation $(1 - \kappa)$ is used for maturation and reproduction. Maturation (in DEB terms) is the process by which resources are burnt to increase the level of complexity of the individual, and hence it is not associated with the

Model component	Specification
Fluxes in mg(dwt) d^{-1}	
Assimilation	$J_A = f J^a_{Am} L^2$
Maintenance	$J_M = J^v_M L^3$
Structural growth	$J_V = y_{VA}(\kappa J_A - J_M)$
Reproduction flux	$J_R = (1-\kappa) J_A$ for $L > L_p$
State variable in mg(dwt)	
Structural body mass	$\frac{d}{dt} W_V = J_V$ with $W_V(0) \approx 0$
Assimilate buffer in egg	$\frac{d}{dt} W_B = -J_A$ with $W_B(0) = W_{B0}$
Reproduction buffer	$\frac{d}{dt} W_R = J_R$ with $W_R(0) = 0$
Conversions	
Volumetric length to dry weight	$W_V = d_V L^3$
Volumetric length to physical length	$L_w = L/\delta_M$
Temperature effect on rate constants	$F_T = \exp\left(\frac{T_A}{T_{ref}} - \frac{T_A}{T}\right)$

Table 1: Equations for the basic DEBkiss model.

Symbol	Description	Value	Unit
Conversion factors			
d_C	carbon weight per body dry weight	0.45	mg mg^{-1}
d_V	dry weight per body volume	0.26	mg mm^{-3}
δ_M	shape-correction nauplii/copepodites	0.50/0.37	[−]
Fixed model parameters			
f	scaled functional response	1	[−]
L_p	volumetric length at puberty	0.53	mm
T_{ref}	reference temperature	283	K
y^c_{AX}	yield of assimilates on food (carbon)	0.80	mg mg^{-1}
y_{BA}	yield of egg buffer on assimilates	0.95	mg mg^{-1}
y_{VA}	yield of structure on assimilates	0.80	mg mg^{-1}
κ	fraction allocation to soma	0.80	[−]
Parameters fitted to growth (ref. 10°C)			
J^a_{Am}	max. area-specific assimilation rate	0.036 (0.034-0.038)	mg mm^{-2} d^{-1}
J^v_M	volume-specific maintenance rate	0.020 (0.018-0.024)	mg mm^{-3} d^{-1}
L_a	volumetric length for stop of growth	0.78 (0.76-0.79)	mm
T_A	Arrhenius temperature	7700 (7400-8000)	K
W_{B0}	dry weight of a single egg	0.72 (0.62-0.86)	μg

Table 2: Parameters of the DEBkiss model as used in this study.

formation of biomass (and not followed as a state variable in DEBkiss). At a certain body size ('puberty'), the investment into maturation is assumed to be completely switched to the reproduction buffer, which is converted into eggs at spawning events. It should be stressed that DEBkiss, in contrast to standard DEB models, does not include a 'reserve' compartment in between assimilation and the κ split.

The state variable for body size in DEBkiss is the structural dry weight W_V (thus excluding storage buffers). The fluxes, however, are based on the volumetric length L, which is the cubic root of structural body volume (L^3). Length of copepods is usually determined as length of the total body or the prosome (L_w). Conversions between these variables are presented in Table 1. It should be stressed that the shape correction coefficient (δ_M) depends on how the length measure is taken (prosome length will require a different value than total body length). To illustrate, for a cube, $\delta_M = 1$ (when L_w refers to the length of a side of the cube), whereas in a cylinder, δ_M will decrease with increasing height/radius (when L_w refers to the height of the cylinder). When the animal does not change in shape during growth (isomorphy), δ_M will be constant over the life cycle.

Starvation occurs when the assimilation flux allocated to the soma (κJ_A) is insufficient to cover the maintenance costs (J_M). The standard rule in DEBkiss is that, first, energy is diverted from the $1 - \kappa$ branch (and thus also from the reproduction buffer). If the $1-\kappa$ branch cannot deliver sufficient energy for maintenance, structure is burnt and the animal will shrink (Jager et al., 2013; Jager and Ravagnan, Acc.). Mortality is not explicitly included in DEBkiss, although a metabolic ageing module (see Kooijman, 2001), or a descriptive model to represent natural mortality, could be added.

For the effects of temperature, we take the Arrhenius relationship (see Table 1); each rate constant is multiplied by the same factor F_T. The temperature correction is applied in fitting of the model to the growth data as well as for the model predictions. For the reference temperature, we selected 10°C, which is at the lower end of the growth data for *C. sinicus* but allows for a smooth comparison with boreal and arctic congeners.

2.2. Modifications for copepods

For the embryo and non-feeding stages, the same equations apply as for the feeding stages, although assimilation occurs from the egg buffer (with $f = 1$) rather than from food. Embryonic development ends when the egg buffer is finished, and at that point ('birth') external feeding becomes possible. In

Calanus species, the egg buffer is still used after hatching to sustain the first two naupliar stages, and hence, hatching precedes 'birth' in the DEB context.

Many copepod species build up a lipid storage of wax esters in the copepodite stages. We propose to view this as a 'reproduction buffer' in DEB terms, and thus as part of the $1-\kappa$ branch. In this view, 'puberty' should be defined by the start of investment into the storage, and the storage dynamics will have no effect on structural growth. We have found no data on the build up or use of storage for *C. sinicus*, so further modification and testing of this part of the model will have to be done in future work. The growth data that we use are based on body length, which is assumed to be a good proxy for structural size. It should be noted that the standard DEB reserve compartment cannot represent this storage as the wax esters are absent in nauplii, and are increasing as fraction of body weight over the copepodite stages until the final moult (see Campbell et al., 2001).

Under constant environmental conditions, the model equations in Table 1 specify von Bertalanffy growth; the growth rate decreases asymptotically to zero as maintenance costs increase with size faster than assimilation. For copepods, however, growth stops after the last moult, well before approaching the asymptotic maximum size. To capture this behaviour, we introduce a final size (L_a), at which investment in structure is stopped ($J_V = 0$). We assume that the assimilation and maintenance fluxes are fixed to the value for the final structural size. After the final moult, *C. sinicus* is able to survive for 3-4 months more, depending on the temperature, under laboratory conditions (Uye, 1988).

For the females, we can calculate the maximum possible reproduction rate that can be fuelled from ingestion alone, by converting all of the assimilated mass minus maintenance to eggs:

$$R = \frac{y_{BA}}{W_{B0}}(J_A - J_M) \tag{1}$$

Reproduction only occurs in the adult stage, so J_A and J_M are calculated using L_a. The predicted reproduction rate is thus constant, for a given food level and temperature. We ignore potential contributions to the egg production from lipid storage or perhaps even structural body tissues. This approach to deal with determinate growth is essentially the same as was used for the standard DEB model by Lika and Kooijman (2003).

2.3. Model predictions

Ingestion rate is often expressed in the literature as daily carbon ration (mg ingested carbon per mg carbon body weight per day), which can be easily calculated from the assimilation flux J_A (introducing the superscript c for carbon-specific mass fluxes):

$$J_X^c = \frac{J_A}{y_{AX}^c L^3 d_V} \tag{2}$$

Neither the carbon content of the organism nor that of the food is needed, as we assume that assimilates have the same composition as biomass, and the assimilation efficiency y_{AX}^c is expressed on carbon basis. The ingestion rate depends on food availability, as J_A depends on f (Table 1). It should be noted that this prediction is based on the structural body weight only, whereas measurements are generally expressed per total body weight (which may include storage).

Respiration is the lump sum of all processes in which carbon is burnt to do work. This obviously includes maintenance costs, but also the investment into maturation (which is assumed to be burnt), and the overhead costs for growth and reproduction. Since we only have respiration data for adults (which do not grow nor mature), we can approximate the respiration rate from maintenance costs only. Expressed as carbon ratio (mg carbon respired per mg carbon body weight per day):

$$J_D^c = \frac{J_M}{d_V L^3} \tag{3}$$

In actively reproducing animals, the respiration rate will be higher, but since we assume a high yield for the translation of assimilates into eggs (y_{BA}), the deviation due to the overhead costs will be small. Like the ingestion rate, this prediction is also based on the structural body weight only, whereas measurements are generally expressed per total body weight. As storage does not require maintenance, the presence of a substantial storage will confound the comparison of model predictions to observations.

2.4. Experimental data from the literature

Data were extracted from graphs in the original publications using the freeware PlotReader (`http://jornbr.home.xs4all.nl/plotreader`). For the model calibration, we used the data collected by Uye (1988). The predictions for ingestion, respiration and reproduction rates were compared to

Temp. (°C)	Start NIII (d)	Start CVI (d)	Estim. NIII (d)	Estim. CVI (d)
20.2	1.77 (0.2)	15.7 (1)	1.64	15.0
17.5	2.03 (0.2)	17.4 (1)	2.09	19.1
15	2.52 (0.2)	24.7 (1)	2.63	24.1
13	3.00 (0.2)	28.1 (1)	3.17	29.0
10.3	4.43 (0.2)	38.6 (1)	4.10	37.5

Table 3: Zero-variate data points used in the optimisation: observed time to reach stages NIII and CVI (taken from Uye, 1988), with assumed s.d. between parentheses. Last two columns show the model estimates for these points after optimisation.

observations taken from Zhang et al. (2006), Zhang et al. (2005) (highest three reproduction rates), Li et al. (2006) (three best food sources), Liu and Wang (2002) (maximum feeding rate), Huo et al. (2008) (four stations with highest reproduction rates), Uye (2000), Li et al. (2013), Li et al. (2004), and Uye and Yamamoto (1995).

2.5. Model calibration

For model calibration, we have data for body length versus time at five temperatures (Uye, 1988). We further constrain the optimisation by including the observed times for reaching 'birth' (start of external feeding at NIII) and 'adulthood' (stop of growth at CVI), summarised in Table 3. In the terminology of Lika et al. (2011), the first data set is uni-variate (paired observations of time and length) and the second zero-variate (single observations on time). Both types of data are included into the overall likelihood function to be maximised.

The data set y for body length versus time needs to be compared to the model predictions $\hat{y}$, following from the parameter set θ. We use the likelihood for the normal distribution where the standard deviation of the residuals is treated as a nuisance parameter and profiled out (see Jager and Zimmer, 2012; Pawitan, 2001). We can combine this with the contribution of the zero-variate data points x; in our case, the observed times for reaching NIII and CVI. For each zero-variate data point x_j, a probability density is calculated of the model prediction for this point $\hat{x}_j$. This probability density follows from the normal distribution f with as mean the zero-variate point x_j and a standard deviation σ_j that has to be provided (arbitrarily) for each point (see Table 3). The overall log-likelihood function (up to a constant) is thus:

$$\ell(\theta|y,x) = -\frac{n}{2}\ln\sum(y_i - \hat{y}_i(\theta))^2 + \sum \ln f(\hat{x}_j(\theta); x_j, \sigma_j^2) \qquad (4)$$

where n is the total number of uni-variate data points. This likelihood function was maximised, and confidence intervals were generated by profiling the likelihood function (see Pawitan, 2001). All model calculations were performed in Matlab R2014a.

3. Results and discussion

3.1. Conversion factors

From the measurements of Pu et al. (2004a) on the dry and wet weight of adults and some CV, we derived a value for the dry weight density (d_V, Table 2). For the carbon content as fraction of the dry weight (d_C), we combined data from Pu et al. (2004a) and Pu et al. (2004b) for adults, which were very similar.

Uye (1988) presents measurements of both body length (prosome for copepodites and carapace for nauplii) and carbon weight from field-collected animals of each developmental stage (except eggs and NI). Using d_C, we can translate carbon weights to dry weights, use d_V to convert these to wet weights, and subsequently take the cubic root to arrive at volumetric length. In Figure 2, the estimated volumetric length is plotted against measured body length. The relationship follows the expected proportionality, but the slope differs between nauplii and copepodites. This indicates that growth in this species is largely isomorphic, apart from the discontinuity between nauplii and copepodites (which also results from the different length measure that was used). The shape correction coefficients (δ_M) for both groups were calculated as the average within each group (Table 2).

The assimilation efficiency on carbon basis was set to a typical value of 80% based on the values proposed for other *Calanus* species (Landry et al., 1984; Tande and Slagstad, 1985).

3.2. Growth curves

Figure 3 shows the fit of the model to the data of Uye (1988) for body size (physical length converted to volumetric length) and developmental time. The conversion to volumetric length allows eggs, nauplii and copepodites to be compared in the same figure. It should be noted that δ_M was calculated

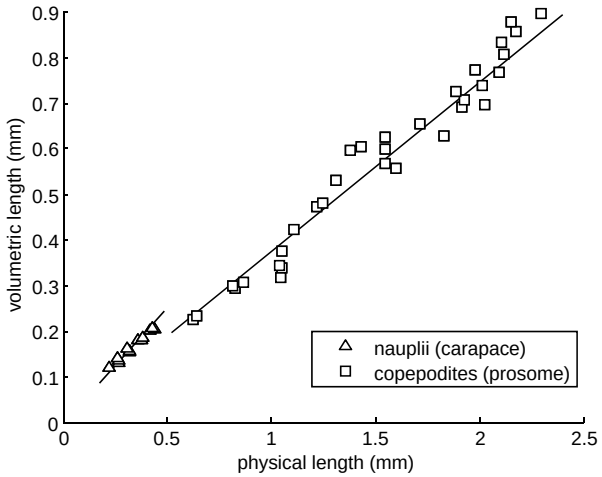

Figure 2: Volumetric length (cubic root of estimated body volume) versus physical length for *Calanus sinicus*. The lines represent the estimate based on the average shape correction coefficients calculated from the data (Table 2).

from field-collected animals whereas these growth data were obtained under laboratory conditions, which constitutes a potential source of bias. The model is fitted to the data at all five temperatures simultaneously (including the zero-variate data in Table 3) by estimating only five model parameters (Table 2).

The value of κ cannot be derived from the growth data alone because of the strict correlation to the specific assimilation rate J^a_{Am}. A lower value of κ will lead to the same investment in growth when J^a_{Am} is increased by the same factor. To identify these parameters uniquely, we would need information about the investment into the $1-\kappa$ branch (see Fig. 1), or reliable estimates for both the ingestion rate and assimilation efficiency. For copepods, reproduction rates are unlikely to provide information about the value for κ as the adults will have to follow a modified rule for energy allocation (as they do not invest in growth). For now, we fixed κ to a typical value of 0.8 (Lika et al., 2011).

Overall, the fit is quite good (Fig. 3), and the data provide sufficient information on the fitted model parameters, as judged from the rather tight confidence intervals (Table 2). The estimated egg weight (which translates to 0.32 μg carbon) is very close to the values reported by Huo et al. (2008) (on average 0.34 μg carbon), although a lower value (0.18 μg carbon) was

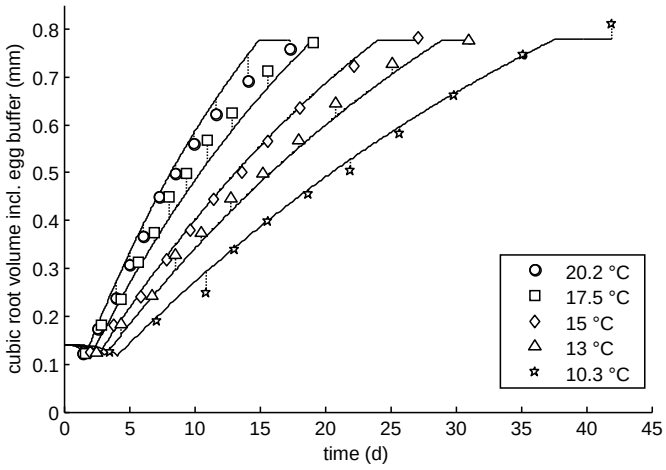

Figure 3: Growth data for *Calanus sinicus* as function of time since deposition of the egg. Body size is expressed as volumetric length (L, cubic root of body volume) including a contribution of the egg buffer for the embryo and non-feeding stages. The observations on body length (converted using the shape correction factors of Table 2) are plotted at the time half-way into the corresponding developmental stage.

reported by Uye and Murase (1997).

At $t = 0$, embryonic development starts. Structural size increases, at the expense of the egg buffer, which leads to a net decrease in the total volume of the organism (part of the egg buffer is lost in respiration due to growth overheads, maintenance and maturation). External feeding starts when the egg buffer is emptied, which should coincide with the start of stage NIII. We placed a zero-variate data point at the development time needed to reach NIII, and the model returns estimates that are very close (Table 3). This implies that the embryonic development is well described by the model with the same parameters as for the feeding stages. This contrasts DEBkiss work with other species (Barsi et al., 2014; Jager et al., 2014b; Jager and Ravagnan, Acc.) where embryonic development was markedly slower than expected from the model.

The growth pattern is consistent with the predicted von Bertalanffy pattern of DEBkiss, up to the final moult. Furthermore, nauplii (after the start of feeding in NIII) and copepodites follow the same curve, when their body size is expressed as volumetric length. The maximum size increases somewhat with decreasing temperature, which is not captured by the model. The reason is not entirely clear, although it is commonly observed for *Calanus*

species, and a differential response to temperature of growth and development has been suggested (Campbell et al., 2001). Growth stops while the animals are still far removed from their asymptotic size (they reach some 55% of the predicted asymptotic length), which implies that the growth pattern is almost linear in time. The estimate for the specific maintenance rate (J_M^v) is almost entirely based on the curvature of the growth pattern. Despite the almost linear growth (on length basis), the estimate for J_M^v has a tight confidence interval (Table 2).

3.3. Model predictions for adults

Even though we calibrated the model to growth data only, DEBkiss describes all mass flows in the organism, and thereby also specifies ingestion, respiration and reproduction (with a few additional parameters). Unfortunately, we could not find data in which these endpoints where determined in conjunction with growth (and lipid storage) under laboratory conditions, and therefore, they were not included into the model fit. We can however obtain a rough indication of the validity of our parameter set by comparing model predictions for ingestion (Eq. 2), respiration (Eq. 3), and potential reproduction rates (Eq. 1), to measured data. All data are from adults, and therefore, only model predictions for adults ($L = L_a$) are shown in Figure 4. For the ingestion and reproduction predictions, three food levels are shown; one *ad libitum* ($f = 1$) and two limiting food levels. The prediction for respiration is based on maintenance costs only, which are assumed not to be influenced by food availability. Due to a general lack of respiration data for *C. sinicus*, we also show the regression equation from Ikeda et al. (2001) for a range of epipelagic marine copepods (converted assuming a respiratory quotient of 0.8).

It should be stressed that most of the data are from field-collected animals, immediately after sampling. The observed rates thus represent animals of unknown age, feeding status, and with an unknown recent temperature history. Only the studies of Li et al. (2006), Liu and Wang (2002) and Uye (2000) were performed under laboratory conditions. Furthermore, most ingestion rates were determined using the gut fluorescence method, which only represents feeding on phytoplankton, thus ignoring the contribution of heterotrophic food sources (Wang et al., 2009; Zhang et al., 2006). And finally, our ingestion and respiration rates are expressed per mg of carbon in structure, whereas measured rates are expressed per total carbon weight, with an unknown contribution of the exoskeleton and lipid storage to the total

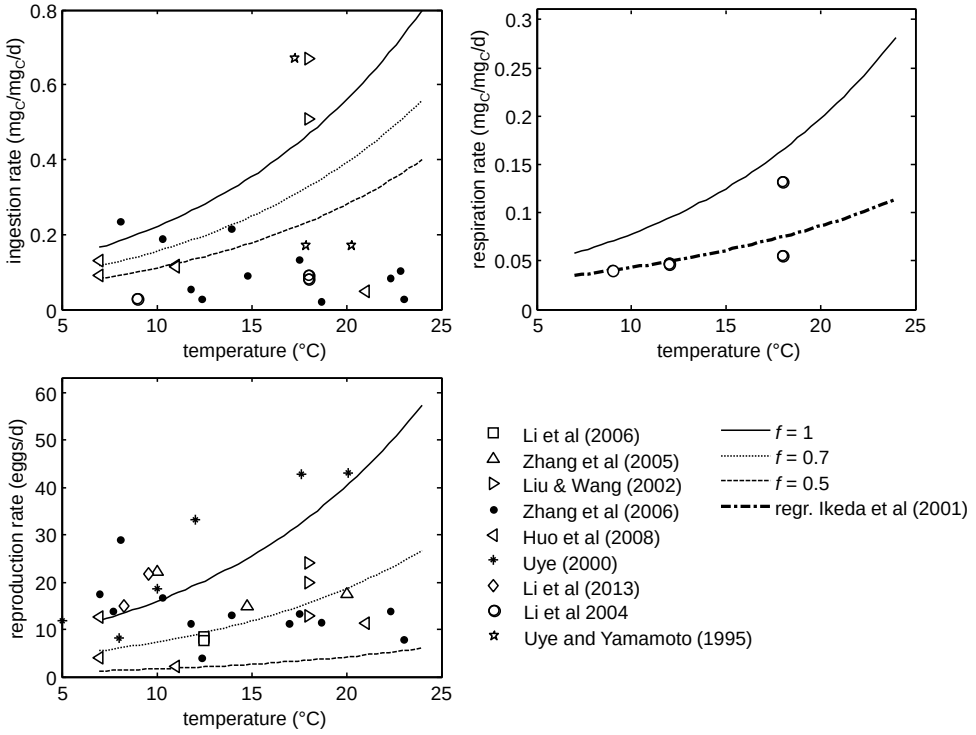

Figure 4: Model predictions for the rates of ingestion, respiration and reproduction, as a function of temperature and food level in adult *Calanus sinicus*. Symbols represent reported values from the literature.

weight. All these factors might explain the considerable scatter, and the fact that most estimates are lower than the maximum predictions ($f = 1$). Nevertheless, this comparison shows that the model calibrated on growth data is able to provide reasonable predictions for other endpoints. The overall consistency of the model predictions with the observations also indicates that the selected default value $\kappa = 0.8$ is a reasonable value for this species. Even though this analysis can give no more than an order-of-magnitude validation, it is important to test the consistency of the model and its parameterisation, and to demonstrate how the various endpoints are connected by the DEBkiss model.

For the respiration rate, the observations and the regression are somewhat lower than the model prediction from our value for maintenance costs only. This could relate to errors in the measurements and/or the conversions applied, or to a contribution of lipid storage to body weight in the data set. Furthermore, it is conceivable that maintenance costs can be reduced in absence of food (for the respiration measurements, animals were kept for 24 hours without food). However, given that our estimate for the maintenance costs is derived from the growth curve, the correspondence to the measured data is striking.

When the ingestion rate is half of the maximum level ($f = 0.5$), reproduction is predicted to be almost zero as the entire assimilation flux would be needed to fulfil the maintenance costs. However, careful consideration of the data sets for which both feeding and reproduction were determined reveals a different pattern: animals for which ingestion is well below the prediction for $f = 0.5$ still reproduce at a substantial rate. This discrepancy may be partially due to an underestimation of the actual ingestion rate (e.g., by ignoring omnivorous feeding, Zhang et al., 2006), and/or an overestimation of the maintenance costs. However, it is possible that these copepods were able to sustain reproduction at low ingestion levels by using lipid storage or even structural body tissues, as was indicated for *C. finmarchicus* (Mayor et al., 2009).

3.4. Evaluation of the modification for copepods

In the introduction, several points are brought forward where the copepod life history deviates from the basic pattern in DEB models: larval stages, determinate growth, and lipid storage. In this section, we evaluate the proposed modification of the standard DEBkiss model.

For the larval stages, we only have to consider that they have a different shape from the copepodites; once we corrected for this (using a different value for δ_M, see Table 2), the body size corresponds well to the model with the same parameters for all life stages (Fig. 3). Embryonic development (which includes the first two non-feeding stages) was also well predicted by the model, without further modifications.

The stop of growth after the final moult was forced onto the model using a maximum size L_a. This, however, implies a deviation from the κ-rule allocation (Fig. 1) in the adult stage (or that κ is switched to a lower value that exactly stops growth at size L_a). In our estimate for the reproduction rate (Eq. 1), we assumed that the entire assimilation flux, minus maintenance costs, could be used for reproduction, which is reasonably consistent with observed reproduction rates (Fig. 4). The metabolic rules for the adults, however, require further detailed study.

The data for *C. sinicus* do not allow an evaluation of the storage dynamics. We tentatively propose to view the lipid storage as a reproduction buffer positioned in the $1 - \kappa$ branch of Figure 1. We can position 'puberty' at the transition from CII to CIII, as this is were lipid storage starts in other *Calanus* species (Lee et al., 2006). The value for L_p in Table 2 is derived from the data of Uye (1988), but not used in the model fits. Clearly, this part of the model also requires further study.

To what extent *C. sinicus* builds up a lipid storage is not entirely clear. The measurements of Uye (1988) on both body length and carbon weight from field-collected animals were used for Figure 2. The linear relationship between prosome length and volumetric length for copepodites suggests that these animals did not build up a considerable lipid storage (assuming that body length is a good proxy for body structure). For field-sampled adults, Wang et al. (2009) found that the oil sac always constituted less than 4% of the total volume (calculated using the shape correction in Table 2). For CV, however, the work of Pu et al. (2004b) shows that these animals have substantially higher C/N ratios than adults, which indicates the presence of lipid storage. Apparently, this species is capable of lipid storage, but we should also consider that *C. sinicus* may have different life-history strategies in different regions or environments (see Pu et al., 2004b). Whether this 'reproduction buffer' can actually be used to fuel reproduction in females of *C. sinicus* is also unclear. Reproduction depends on feeding, whereas the lipid storage is likely only used to fuel maintenance in times of food shortage (Wang et al., 2009).

4. Conclusions

The DEBkiss model provides a simple and generic framework for the energy budget of animals. The present analysis indicates that application to calanoid copepods can depart from the same basic model structure, with limited modifications to address the specifics of the copepod life history as outlined in the introduction. With these modifications, the model could be parameterised for *C. sinicus* using a limited amount of biological information. The calibrated model was able to provide an adequate representation of growth and development (Fig. 3), as well as ingestion, respiration and egg production (Fig. 4). Our DEBkiss model represents an enormous simplification of the biological complexity of the calanoid life cycle. Clearly, many of the 'details' on moulting, composition, gonad development, etcetera, are lost or lumped into more abstract energy fluxes (e.g., moulting costs are considered to be part of the growth overheads). Such simplification, however, is highly advantageous for many research questions. Firstly, the model is useful to test whether observed (or expected) life-history traits are quantitatively consistent with the conservation laws. Secondly, simple DEB-based models have proven to be extremely useful for applied ecology, such as in the interpretation of toxic effects (Jager and Zimmer, 2012), or as basis for physiologically-structured population modelling (Jager et al., 2014a).

Several important issues remain to be addressed, specifically the dynamics of the lipid storage (both its build-up and its use) and the metabolic rules for the adult stage. Elucidating these rules will be essential to include the energetics of resting phases or diapause in the life cycle (Li et al., 2004), but also to interpret the response to stressors, such as pollution (Klok et al., 2012), and its consequences for population viability. These questions are amenable to experimental work, and the current DEBkiss analysis can aid in the design of such studies. We can expect that related species have similar parameters values, and the current parameterisation therefore forms a solid starting point for future work on this and other *Calanus* species.

5. Acknowledgements

This work was conducted as part of the ENERGYBAR project, financed by the Research Council of Norway (grant no. 225314/E40).

References

Barsi, A., Jager, T., Collinet, M., Lagadic, L., Ducrot, V., 2014. Considerations for test design to accommodate energy-budget models in ecotoxicology: a case study for acetone in the pond snail *Lymnaea stagnalis*. Environmental Toxicology and Chemistry 33, 1466–1475.

Campbell, R.G., Wagner, M.M., Teegarden, G.J., Boudreau, C.A., Durbin, E.G., 2001. Growth and development rates of the copepod *Calanus finmarchicus* reared in the laboratory. Marine Ecology Progress Series 221, 161–183.

Hamda, N.T., 2014. Mechanistic models to explore combined effects of toxic chemicals and natural stressing factors: case study on springtails. PhD thesis, Jagiellonian University, Krakow/VU University Amsterdam (http://hdl.handle.net/1871/50121).

Hartnoll, R.G., 2001. Growth in crustacea - twenty years on. Hydrobiologia 449, 111–122.

Huo, Y.Z., Wang, S.W., Sun, S., Li, C.L., Liu, M.T., 2008. Feeding and egg production of the planktonic copepod *Calanus sinicus* in spring and autumn in the Yellow Sea, China. Journal of Plankton Research 30, 723–734.

Ikeda, T., Kanno, Y., Ozaki, K., Shinada, A., 2001. Metabolic rates of epipelagic marine copepods as a function of body mass and temperature. Marine Biology 139, 587–596.

Jager, T., Barsi, A., Hamda, N.T., Martin, B.T., Zimmer, E.I., Ducrot, V., 2014a. Dynamic energy budgets in population ecotoxicology: applications and outlook. Ecological Modelling 280, 140–147.

Jager, T., Gudmundsdóttir, E.M., Cedergreen, N., 2014b. Dynamic modeling of sub-lethal mixture toxicity in the nematode *Caenorhabditis elegans*. Environmental Science & Technology 48, 7026–7033.

Jager, T., Martin, B.T., Zimmer, E.I., 2013. DEBkiss or the quest for the simplest generic model of animal life history. Journal of Theoretical Biology 328, 9–18.

Jager, T., Ravagnan, E., Acc. Parameterising a generic model for the dynamic energy budget of Antarctic krill, *Euphausia superba*. Marine Ecology Progress Series DOI 10.3354/meps11098.

Jager, T., Zimmer, E.I., 2012. Simplified Dynamic Energy Budget model for analysing ecotoxicity data. Ecological Modelling 225, 74–81.

Klok, C., Hjorth, M., Dahllöf, I., 2012. Qualitative use of Dynamic Energy Budget theory in ecotoxicology. Case study on oil contamination and Arctic copepods. Journal of Sea Research 73, 24–31.

Kooijman, S.A.L.M., 2001. Quantitative aspects of metabolic organization: a discussion of concepts. Philosophical Transactions of the Royal Society of London B 356, 331–349.

Landry, M.R., Hassett, R.P., Fagerness, V., Downs, J., Lorenzen, C.J., 1984. Effect of food acclimation on assimilation efficiency of *Calanus pacificus*. Limnology and Oceanography 29, 361–364.

Lee, R.F., Hagen, W., Kattner, G., 2006. Lipid storage in marine zooplankton. Marine Ecology Progress Series 307, 273–306.

Li, C., Sun, S., Wang, R., Wang, X., 2004. Feeding and respiration rates of a planktonic copepod (*Calanus sinicus*) oversummering in Yellow Sea Cold Bottom Waters. Marine Biology 145, 149–157.

Li, C.L., Yang, G., Ning, J., Sun, J., Yang, B., Sun, S., 2013. Response of copepod grazing and reproduction to different taxa of spring bloom phytoplankton in the Southern Yellow Sea. Deep-Sea Research Part II-Topical Studies in Oceanography 97, 101–108.

Li, J., Sun, S., Li, C.L., Zhang, Z., Tao, Z.C., 2006. Effects of single and mixed diatom diets on the reproduction of copepod *Calanus sinicus*. Acta Hydrochimica Et Hydrobiologica 34, 117–125.

Lika, K., Kearney, M.R., Freitas, V., Van der Veer, H.W., Van der Meer, J., Wijsman, J.W.M., Pecquerie, L., Kooijman, S.A.L.M., 2011. The "covariation method" for estimating the parameters of the standard Dynamic Energy Budget model I: philosophy and approach. Journal of Sea Research 66, 270–277.

Lika, K., Kooijman, S.A.L.M., 2003. Life history implications of allocation to growth versus reproduction in dynamic energy budgets. Bulletin of Mathematical Biology 65, 809–834.

Liu, S., Wang, W.X., 2002. Feeding and reproductive responses of marine copepods in South China Sea to toxic and nontoxic phytoplankton. Marine Biology 140, 595–603.

Mayor, D.J., Anderson, T.R., Pond, D.W., Irigoien, X., 2009. Egg production and associated losses of carbon, nitrogen and fatty acids from maternal biomass in *Calanus finmarchicus* before the spring bloom. Journal of Marine Systems 78, 505–510.

Nisbet, R.M., Muller, E.B., Lika, K., Kooijman, S.A.L.M., 2000. From molecules to ecosystems through dynamic energy budget models. Journal of Animal Ecology 69, 913–926.

Pawitan, Y., 2001. In all likelihood: statistical modelling and inference using likelihood. Oxford University Press, Oxford, UK.

Pu, X.M., Sun, S., Yang, B., Ji, P., Zhang, Y.S., Zhang, F., 2004a. The combined effects of temperature and food supply on *Calanus sinicus* in the southern Yellow Sea in summer. Journal of Plankton Research 26, 1049–1057.

Pu, X.M., Sun, S., Yang, B., Zhang, G.T., Zhang, F., 2004b. Life history strategies of *Calanus sinicus* in the southern Yellow Sea in summer. Journal of Plankton Research 26, 1059–1068.

Saraiva, S., van der Meer, J., Kooijman, S.A.L.M., Witbaard, R., Philippart, C.J.M., Hippler, D., Parker, R., 2012. Validation of a Dynamic Energy Budget (DEB) model for the blue mussel *Mytilus edulis*. Marine Ecology Progress Series 463, 141–158.

Tande, K.S., Slagstad, D., 1985. Assimilation efficiency in herbivorous aquatic organisms - the potential of the ratio method using 14C and biogenic silica as markers. Limnology and Oceanography 30, 1093–1099.

Uye, S., 1988. Temperature-dependent development and growth of *Calanus sinicus* (Copepoda, Calanoida) in the laboratory. Hydrobiologia 167, 285–293.

Uye, S., 2000. Why does *Calanus sinicus* prosper in the shelf ecosystem of the Northwest Pacific Ocean? Ices Journal of Marine Science 57, 1850–1855.

Uye, S., Murase, A., 1997. Relationship of egg production rates of the planktonic copepod *Calanus sinicus* to phytoplankton availability in the Inland Sea of Japan. Plankton Biology & Ecology 44, 3–11.

Uye, S., Yamamoto, F., 1995. In situ feeding of the planktonic copepod *Calanus sinicus* in the Inland Sea of Japan, examined by the gut fluorescence method. Bulletin of Plankton Society of Japan 42, 123–139.

Wang, S.W., Li, C.L., Sun, S., Ning, X.R., Zhang, W.C., 2009. Spring and autumn reproduction of *Calanus sinicus* in the Yellow Sea. Marine Ecology Progress Series 379, 123–133.

Zhang, G.T., Li, C.L., Sun, S., Zhang, H.Y., Sun, J., Ning, X.R., 2006. Feeding habits of *Calanus sinicus* (Crustacea: Copepoda) during spring and autumn in the Bohai Sea studied with the herbivore index. Scientia Marina 70, 381–388.

Zhang, G.T., Sun, S., Zhang, F., 2005. Seasonal variation of reproduction rates and body size of *Calanus sinicus* in the Southern Yellow Sea, China. Journal of Plankton Research 27, 135–143.